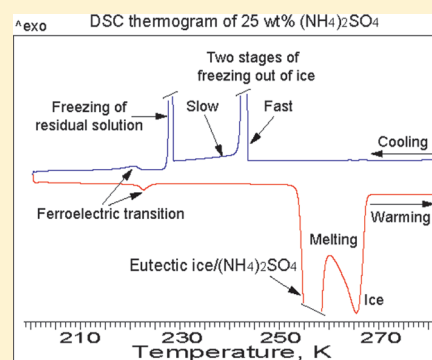


# Impact of Substrate, Aging, and Size on the Two Freezing Events of $(\text{NH}_4)_2\text{SO}_4/\text{H}_2\text{O}$ Droplets

Anatoli Bogdan<sup>\*,†,‡,§</sup> and Thomas Loerting<sup>†</sup><sup>†</sup>Institute of Physical Chemistry, University of Innsbruck, Innrain 52a, A-6020 Innsbruck, Austria<sup>‡</sup>Laboratory of Polymer Chemistry, Department of Chemistry, P.O. Box 55, University of Helsinki, FI-00014 Finland<sup>§</sup>Department of Physics, P.O. Box 48, University of Helsinki, FI-00014 Finland

**ABSTRACT:** Below the eutectic point of  $T_e \approx 254.5$  K, millimeter-scaled  $(\text{NH}_4)_2\text{SO}_4/\text{H}_2\text{O}$  droplets placed on an Al substrate produce two heterogeneous freezing events: the freezing out of pure ice at  $T_{\text{ice}}$  and the subsequent freezing of a residual freeze-concentrated solution at  $T_{\text{res}}$ . Whether the appearance of  $T_{\text{ice}}$  and  $T_{\text{res}}$  is governed by the substrate, aging, and the size of droplets was unclear and is investigated here. We present differential scanning calorimetry results of the study of freezing aqueous 25 wt %  $(\text{NH}_4)_2\text{SO}_4$  droplets placed on 11 substrates of different surface properties, including four oil–surfactant mixtures. The analysis shows the following: (i) Independent of substrates, the two freezing events always appear below  $T_e$ , and  $T_{\text{ice}}$  is always higher than  $T_{\text{res}}$ . (ii) The freezing out of ice consists of a fast stage, during which the majority of ice is formed, and a sluggish stage, during which the ice crystallization continues until the residual solution starts freezing. (iii)  $T_{\text{res}}$  is more sensitive to surface properties than  $T_{\text{ice}}$ ; that is, the second freezing event related

to the residual solution takes place heterogeneously. (iv) The heterogeneous freezing of the residual solution most likely begins from the nucleation of  $(\text{NH}_4)_2\text{SO}_4$  crystals. (v) The lanolin surfactant impacts the freezing behavior of 25 wt %  $(\text{NH}_4)_2\text{SO}_4$  droplets; that is, in contrast to the past belief, lanolin can also impact the freezing behavior of emulsified droplets. (vi) The measurements of 2.5 month-old 25 wt %  $(\text{NH}_4)_2\text{SO}_4$  droplets show that there is no reaction between lanolin and  $\text{NH}_4^+$  or  $\text{SO}_4^{2-}$ . (vii) A 20-fold increase of the mass of 25 wt %  $(\text{NH}_4)_2\text{SO}_4$  droplets does not impact the appearance of  $T_{\text{ice}}$  and  $T_{\text{res}}$ .



## 1. INTRODUCTION

The understanding of the freezing behavior of aqueous solutions is important for different natural and industrial processes.<sup>1–8</sup> The freezing of bulk binary solutions is usually viewed as follows: dilute solutions freeze above the eutectic point, and a phase separation occurs into ice and a freeze-concentrated residual solution. The latter is formed by the expulsion and segregation of solute ions during the freezing out of ice. As the temperature continues to decrease, the concentration of the residual solution continues to increase along the ice/solution equilibrium line until the eutectic point is reached. When solutions are cooled below the eutectic point, they freeze to a solid mixture of ice and salt-hydrate crystals.<sup>7</sup> In contrast to bulk solutions, micrometer-scaled droplets are easily cooled much below the eutectic point.<sup>9–12</sup> Recently, it has been reported that larger, millimeter-scaled  $(\text{NH}_4)_2\text{SO}_4/\text{H}_2\text{O}$  droplets of a subeutectic composition can be also cooled below the eutectic point of  $T_e \approx 254.5$  K, which is not consistent with the “usual view” explained above.<sup>13,14</sup> The millimeter-scaled  $(\text{NH}_4)_2\text{SO}_4/\text{H}_2\text{O}$  droplets freeze in two steps: at first, pure ice freezes out at  $T_{\text{ice}}$ , and then a residual freeze-concentrated solution freezes at  $T_{\text{res}} < T_{\text{ice}}$ . Because the two freezing events are observed in  $(\text{NH}_4)_2\text{SO}_4/\text{H}_2\text{O}$  droplets placed on an aluminum substrate, one may suggest that the Al substrate could be responsible for this behavior. In aqueous droplets, which are in

contact with a surface, the freezing out of ice occurs heterogeneously, and different surfaces, having different ice nucleation efficiencies, would produce different heterogeneous freezing temperatures.<sup>4</sup> However, it has not been investigated so far whether substrates can govern the freezing of a residual solution and, consequently, impact on the mutual distribution of the two freezing temperatures  $T_{\text{ice}}$  and  $T_{\text{res}}$ .

Millimeter-scaled droplets stand in a midposition between bulk solutions and emulsified micrometer-scaled droplets. The understanding of the heterogeneous freezing of millimeter-scaled droplets can be important because, in nature, aqueous solutions are often attached to different surfaces, for example, in soils, rocks, trees, etc.<sup>15</sup> It is obvious that the concentration and acidity of the solution increase as ice freezes out.<sup>16,17</sup> The rate of some chemical reactions is increased in the unfrozen residual solution.<sup>6,18–20</sup> In frozen residual solutions, the chemical reactions may, on the other hand, be extremely slow or suppressed entirely. Whether the residual solution is frozen or not may also impact on natural glacial systems. The glacial systems are formed by the freezing of carbonate-bearing solutions and/or by refreezing of meltwater that has contacted rock debris on or within ice

Received: January 24, 2011

Revised: April 26, 2011

Published: May 06, 2011

sheets.<sup>21</sup> The presence of unfrozen residual solution between the grain-scaled ice microstructures is also important in environmental issues, such as the evolution, rheology, and transport properties of mountain glaciers, polar ice caps, and sea ice that are important in a time of changing climate. The understanding of the freezing behavior of sub- and micrometer-scaled aqueous droplets is important for the atmosphere.<sup>5,10–14,22–25</sup> Whether a residual unfrozen solution exists around cloud ice particles, which are formed after the freezing of atmospheric aerosol droplets—the precursors of cirrus and polar stratospheric clouds (PSCs)—can have important consequences for atmospheric chemistry (for example, the change of the rate of polar stratospheric and upper-tropospheric ozone destruction),<sup>10</sup> the change of the radiative properties of cirrus,<sup>24</sup> and the uptake of water vapor (dominant greenhouse gas) by cirrus ice particles.<sup>5,25</sup> Because cirrus clouds cover about 30% of the globe, the microphysics of ice cirrus clouds may be an important factor impacting on the climate and, therefore, should be taken into account in climate models.

The study of the freezing behavior of sub- and micrometer-scaled aqueous droplets is convenient using emulsions. In this case, one studies large populations of emulsified droplets and statistical trends rather than single droplets. Large populations of emulsified droplets are often considered as an analogue of atmospheric droplets—the precursors of upper tropospheric (UT) cirrus and PSCs.<sup>5,10–12</sup> Their freezing behavior is studied in order to get insight into the formation mechanisms and microphysical properties of cirrus and PSCs. Although the sizes and concentrations of atmospheric and emulsified droplets can be similar, their environment is completely different. In an emulsion, the droplets are dispersed in an oil/surfactant matrix, whereas in the atmosphere, they are suspended in the gaseous phase. It is thought that the oil/surfactant matrix does not significantly influence the freezing behavior of emulsified aqueous droplets and, therefore, their freezing can be considered as homogeneous.<sup>22</sup> However, the impact of the oil/surfactant matrix on the freezing behavior of emulsified droplets and, in particular, on the appearance of the two freezing events of  $T_{ice}$  and  $T_{res}$  has not been investigated. Also, the impact of the size of aqueous droplets and the aging of the solution/substrate interface on the appearance of  $T_{ice}$  and  $T_{res}$  has not been investigated. The aim of this paper is to present the DSC results of the study of the impact of different substrates, the mass (size) of droplets, and the aging of the solution/surfactant interface on the appearance of  $T_{ice}$  and  $T_{res}$  during the cooling of millimeter-scaled 25 wt %  $(NH_4)_2SO_4$  droplets.

## 2. EXPERIMENTAL SECTION

In freezing measurements, we use aqueous 25 wt %  $(NH_4)_2SO_4$  droplets with a diameter of  $\sim 0.3$ – $2$  mm (mass of  $\sim 0.7$ – $18$  mg). The bulk 25 wt %  $(NH_4)_2SO_4$  solution is prepared by mixing 99.99%  $(NH_4)_2SO_4$  crystals (Sigma Aldrich) with the corresponding amount of ultrapure water. The concentration of 25 wt %  $(NH_4)_2SO_4$  is below the eutectic concentration of  $\sim 40$  wt %  $(NH_4)_2SO_4$ . On cooling, 25 wt %  $(NH_4)_2SO_4$  droplets produce two distinct freezing events that are clearly seen as two exothermic peaks in DSC thermograms.<sup>13,14</sup> Measuring droplets of constant concentration allows us to investigate the effect of substrates, aging, and size of droplets on their freezing behavior without having to consider effects (e.g., freezing temperature shifts) caused by the variation of concentration.

The 25 wt %  $(NH_4)_2SO_4$  droplets are placed on 11 substrates: (i) gold (Au), (ii) aluminum (Al), (iii) hydrophobic halocarbon grease series 28LT, (iv) hydrophobic lanolin wax (Sigma Aldrich), (v) hydrophilic halocarbon oil series 0.8 (Halocarbon Products Corp.), (vi) mineral oil, (vii) a superhydrophobic semifluorinated block copolymer with a contact angle for water larger than  $150^\circ$ , and (viii) four oil/surfactant matrixes (mixtures) that are used for the preparation of emulsions. The oil/surfactant matrixes are mixtures of (i) 80 wt % halocarbon oil series 0.8 + 20 wt % lanolin, (ii) 77 wt % mineral oil + 23 wt % lanolin, (iii) 93 wt % halocarbon oil series 0.8 + 7 wt % Span 65, and (iv) a 1:1 mixture of methylcyclopentane/methylcyclohexane (Merck) + 7 wt % Span 65.<sup>23</sup> Lanolin wax is a natural organic surfactant that consists of cholesterol, wool alcohols, and the esters derived from several fatty acids. Span65 is a nonionic surfactant. Lanolin and Span65 are widely used for the preparation of emulsions. Halocarbon oil series 0.8 is a low molecular mass polymer of chlorotrifluoroethylene (PCTFE) and is chemically inert to practically all acids, alkalis, and oxidizing agents. A mineral oil is composed mainly of alkanes (typically 15–40 carbons) and cyclic paraffins. Standard gold and aluminum DSC crucibles with a volume of  $40 \mu L$  were used as Au and Al substrates. Because metallic Al, being exposed to atmospheric oxygen, almost instantly becomes covered with an oxide  $Al_2O_3$  film of  $\sim 4$  nm in thickness, the droplets are, in fact, in contact with  $Al_2O_3$ . The substrates of grease, lanolin, a semifluorinated block copolymer, halocarbon and mineral oils, and four oil/surfactant matrixes are thin films on the bottom and walls of Al crucibles. The film of semifluorinated block copolymer is prepared according to the procedure described elsewhere.<sup>26</sup> On the substrates of Au, Al ( $Al_2O_3$ ), halocarbon grease, and lanolin wax, 25 wt %  $(NH_4)_2SO_4$  droplets form approximately a hemisphere with a contact angle of  $\sim 70$ – $80^\circ$ . On the surface of the semifluorinated block copolymer, the droplets have a contact angle of  $\sim 90$ – $100^\circ$ . On the hydrophilic films of halocarbon oil and four oil/surfactant matrixes, the 25 wt %  $(NH_4)_2SO_4$  solution forms a thin film. The large distribution of contact angles, from  $0^\circ$  on hydrophilic substrates to  $\sim 90$ – $100^\circ$  on the semifluorinated block copolymer, indicates that the substrates used possess different surface properties.

The freezing measurements were performed with a Mettler Toledo DSC 822 calorimeter. The calorimeter is well-calibrated and reproduces the melting points of indium (429.75 K), water (273.15 K), and heptane (182 K) to better than  $\pm 0.3$ – $0.4$  K. The measurements were performed at a scanning cooling and warming rates of 3 K/min between 278 and 133 K. A number of repeated measurements were done to verify the reproducibility of results. For example, we performed more than 25 measurements of 25 wt %  $(NH_4)_2SO_4$  droplets placed on a halocarbon oil + lanolin mixture (matrix), more than 20 measurements of droplets placed on Al ( $Al_2O_3$ ), and from 3 to 15 measurements on each of the other substrates. The repeated measurements were of two types: (i) on the same 25 wt %  $(NH_4)_2SO_4$  droplets and (ii) on different 25 wt %  $(NH_4)_2SO_4$  droplets. In the case of Au crucibles, the repeated measurements were on the same droplet. Before each measurement, the Au crucible was shaken in order to move the droplet to another position. Au crucibles are expensive and such a procedure allows performing repeated measurements using one Au crucible.

To verify the stability of the  $(NH_4)_2SO_4/H_2O$ /lanolin interface, a part of the measurements was performed on the same “fresh” and “aged” droplets that were placed on lanolin and

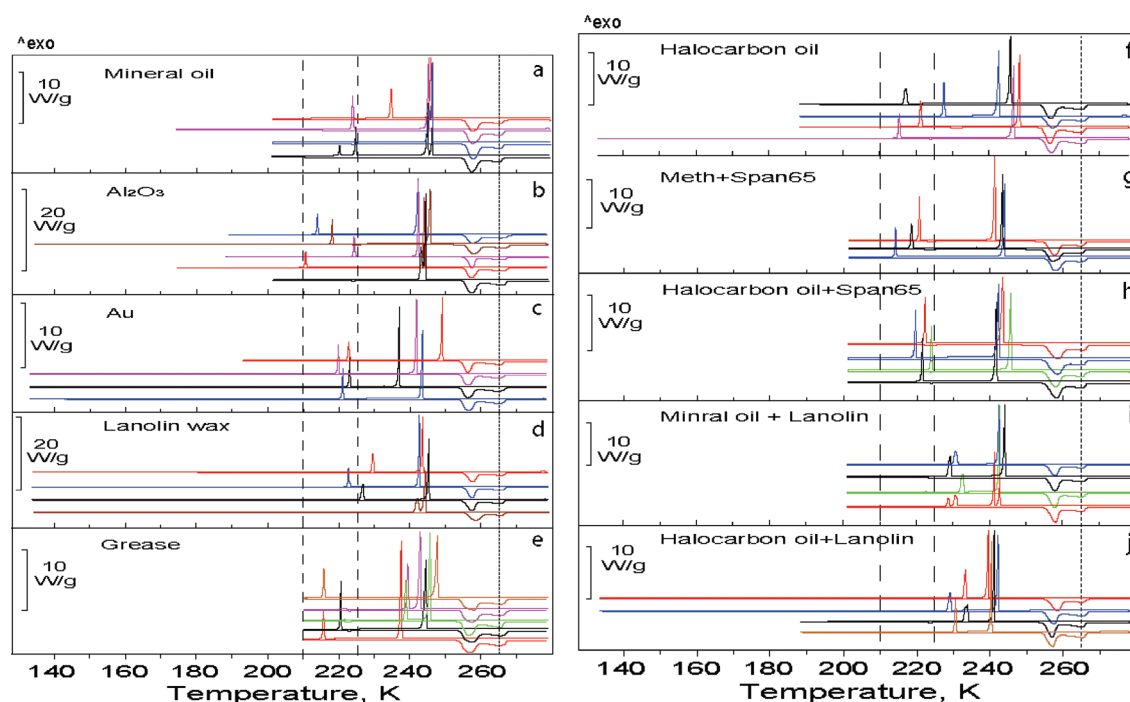


**Figure 1.** DSC cooling/warming thermograms of 25 wt %  $(\text{NH}_4)_2\text{SO}_4$  droplets placed on 10 different substrates: (a) mineral oil, (b) Al ( $\text{Al}_2\text{O}_3$ ), (c) Au, (d) lanolin wax, (e) halocarbon grease, (f) halocarbon oil series 0.8, and four oil–surfactant mixtures of (g) a 1:1 mixture of methylcyclopentane/methylcyclohexane + 7 wt % Span65, (h) 93 wt % halocarbon oil series 0.8 + 7 wt % Span65, (i) 77 wt % mineral oil + 23 wt % lanolin, and (j) 80 wt % halocarbon oil series 0.8 + 20 wt % lanolin. The large and small exothermic peaks directed upward are due to the heat of fusion released during the freezing out of pure ice and the freezing of a residual solution, respectively. The endothermic peaks directed downward are produced by the heat of fusion absorbed during the melting of eutectic ice/ $(\text{NH}_4)_2\text{SO}_4$  (cold peak) and pure ice, respectively. The lowest black thermogram in (a) and the lowest red thermogram in (i) were obtained from two droplets placed in one crucible. Therefore, these thermograms contain four freezing peaks. The dotted line indicates the peak melting temperature of ice  $T_{\text{ice,m}} \approx 265$  K. The two dashed lines indicate the temperature region of  $\sim 210$ – $225$  K (see text for details). The mass of droplets is  $\sim 5$ – $12$  mg. The cooling/warming rate is 3 K/min. The scaled bars denote the heat flow through droplets.

oil/lanolin substrates. “Fresh” means that the measurements were completed within less than 2 h after the droplets were put in contact with the lanolin-containing substrates. “Aged” means that the droplets were in contact with the lanolin-containing substrates for more than 2.5 months before the second measurements started. The weighing showed that the mass of “fresh” and “aged” droplets was the same.

The time needed for the loading of droplets into DSC crucibles and their subsequent hermetic cold sealing was less than  $\sim 15$  s. The measurements of the droplets with a mass smaller than 1 mg (see Figure 11) showed that the amount of evaporated water during the loading was large enough to change the concentration. The increase of the concentration is easily detected by the shift of the melting temperature of ice to colder temperature in DSC thermograms.

### 3. RESULTS AND DISCUSSION

**3.1. Two Freezing Events,  $T_{\text{ice}}$  and  $T_{\text{res}}$ .** Figure 1 presents the collection of typical thermograms obtained during the cooling/warming of 25 wt %  $(\text{NH}_4)_2\text{SO}_4$  droplets placed on 10 substrates of different surface properties. (The 11th substrate is discussed in section 3.10.) It is seen that independent of the substrates, all cooling thermograms contain two freezing events: the freezing out of pure ice,  $T_{\text{ice}}$  (large exothermic peaks), and the freezing of a residual solution,  $T_{\text{res}}$  (small exothermic peaks). In the warming thermograms, the two melting events of  $T_{\text{res,m}}$  and  $T_{\text{ice,m}}$  are due to the melting of the eutectic mixture of ice/ $(\text{NH}_4)_2\text{SO}_4$

(cold endothermic peaks) and pure ice, respectively.<sup>13</sup> Note that the lowest black and red thermograms in Figure 1a,i, respectively, contain four freezing peaks: two large peaks of  $T_{\text{ice}}$  and two small peaks of  $T_{\text{res}}$ . These thermograms are obtained from two separate droplets placed in one Al crucible. However, the corresponding warming thermograms contain only two melting events as in the warming thermograms of single droplets. Figure 1 shows that, in all thermograms, the peak melting temperatures are constant,  $T_{\text{res,m}} \approx 257$  K and  $T_{\text{ice,m}} \approx 265$  K. It should be recalled that, by definition, the eutectic melting temperature of  $T_e \approx 254.5$  K is the onset of the melting of the eutectic ice/ $(\text{NH}_4)_2\text{SO}_4$  mixture.<sup>13,27</sup> Indeed, the onset temperatures extracted from the thermograms in Figure 1 do not deviate by more than  $\pm 0.5$  K from 254.5 K. Figure 1 shows that, independent of the surface properties of the substrates, the two freezing events  $T_{\text{ice}}$  and  $T_{\text{res}}$  always fall well below the  $T_e$ .

The fact that the peak melting temperature of ice,  $T_{\text{ice,m}} \approx 265$  K, is the same in all thermograms indicates that the overall concentration of 25 wt %  $(\text{NH}_4)_2\text{SO}_4$  is not changed on the time-scale of measurements less than 2 h (see the Experimental Section). The  $T_{\text{ice,m}}$  agrees with the melting point of 25 wt %  $(\text{NH}_4)_2\text{SO}_4$  solution in the equilibrium phase diagram of  $(\text{NH}_4)_2\text{SO}_4/\text{H}_2\text{O}$ .<sup>13,27</sup> Further, Figure 1 shows that there is no indication of other freezing events on cooling from  $T_{\text{res}}$  to 133 K. On subsequent warming, there are no melting events up to  $T_e$ . The magnification of the low-temperature parts of the cooling/warming thermograms shows no indication of glass transition that usually manifests itself by a step in a baseline. In ref 14, we

reported that micrometer-scaled emulsified  $(\text{NH}_4)_2\text{SO}_4/\text{H}_2\text{O}$  droplets produce a subtle glass transition at  $T_g \approx 172$  K. This is accounted for by the small size of droplets that are capable of producing the glass transition at cooling rate as small as 3 K/min. It is possible that a very large cooling rate would produce a glass transition also in millimeter-scaled droplets. The interplay between the appearance of the glass transition, the size of glass forming liquids, and the applied cooling rate is briefly discussed in ref 25. Because there is no transition below  $T_{\text{res}}$ , some measurements were performed down to only slightly below  $T_{\text{res}}$  (Figure 1).

In the temperature region between  $T_{\text{ice}}$  and  $T_{\text{res}}$ , the droplets (films) are in the mixed-phase state: pure ice and a residual freeze-concentrated  $(\text{NH}_4)_2\text{SO}_4/\text{H}_2\text{O}$  solution. Most likely, the residual solution is in contact with both ice and substrates, as is schematically shown in Figure 2. The residual solution wets and coats ice and, therefore, may reach substrates. Our numerous optical microscopy observations show that, on hydrophobic substrates, aqueous droplets, including  $(\text{NH}_4)_2\text{SO}_4/\text{H}_2\text{O}$  droplets, always preserve a half-spherical form after freezing (not shown). Although the optical microscopy observations show the presence of a residual solution on the surface of droplets between  $T_{\text{ice}}$  and  $T_{\text{res}}$  (not shown), we do not completely exclude the possibility that some of the residual solution may exist inside ice as “veins”. However, because the size of droplets is small (less than 2 mm), the amount of the residual solution in the “veins” may be very small. Because droplets (films) are placed on substrates, the freezing out of pure ice occurs heterogeneously. Being in contact with substrates and ice, the residual solution may also freeze heterogeneously. Below the impact of substrates on the two freezing events will be analyzed separately for  $T_{\text{ice}}$  and  $T_{\text{res}}$ .

**3.2. Impact of Substrates on  $T_{\text{ice}}$ .** Figure 1 demonstrates that the average heterogeneous freezing temperatures of ice  $T_{\text{ice},n}^{\text{avr}}$  are quite similar despite that the substrates possess different

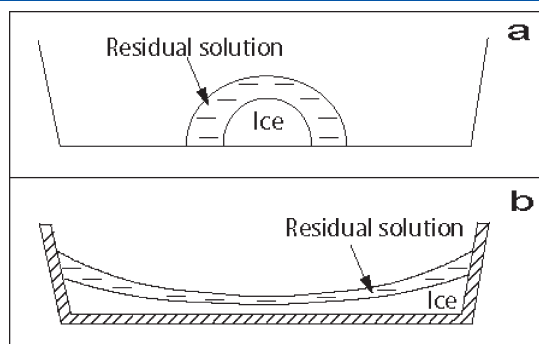


**Figure 2.** Scheme of partly frozen (a) 25 wt %  $(\text{NH}_4)_2\text{SO}_4$  droplets placed on hydrophobic substrates and (b) 25 wt %  $(\text{NH}_4)_2\text{SO}_4$  films formed on hydrophilic substrates.

surface properties. A subscript  $n$  varies between 1 and 10 according to the letters denoting the panels of Figure 1a–j. The scattering of individual  $T_{\text{ice},n}$ 's around the  $T_{\text{ice},n}^{\text{avr}}$  is different, being the smallest for mineral oil (Figure 1a) and the largest for the Au substrate (Figure 1c). Table 1 is presented to show the average freezing temperatures of  $T_{\text{ice},n}^{\text{avr}}$  and their standard deviations of  $\sigma_n$ . The  $T_{\text{ice},n}^{\text{avr}}$ 's and  $\sigma_n$ 's have been calculated over all thermograms obtained on substrates, not only over those ones collected in Figure 1. In Table 1, the capital letter  $N$  is the number of measurements performed on each substrate. For a better demonstration, the  $T_{\text{ice},n}^{\text{avr}}$  and  $\sigma_n$  are also presented in Figure 3. It is seen that the difference between the warmest  $T_{\text{ice},f}^{\text{avr}}$  obtained on halocarbon oil and the coldest  $T_{\text{ice},j}^{\text{avr}}$  obtained on the halocarbon oil/lanolin mixture is only  $\sim 6$  K. Figure 3 shows that the  $T_{\text{ice},n}^{\text{avr}}$ 's can be divided into two groups: a “warm” group in which the warmer  $T_{\text{ice},n}^{\text{avr}}$ 's are obtained on the five substrates of a, b, c, e, and f (see Table 1 and Figure 3) and a “cold” group in which the colder  $T_{\text{ice},n}^{\text{avr}}$ 's are obtained on the substrates denoted by d, g, h, i, j, and k in Figure 3. The letter k denotes a semifluorinated block copolymer substrate. The phase transitions of 25 wt %  $(\text{NH}_4)_2\text{SO}_4$  droplets placed on the semifluorinated block copolymer will be discussed in section 3.10.

Large bulk aqueous solutions, which are made of not sufficiently pure components, freeze heterogeneously owing to immersed ice nuclei that can be nanometer-sized dust particles or/and other solid impurity inclusions.<sup>4</sup> Although our millimeter-scaled droplets are considerably smaller than bulk solutions, they nevertheless are much larger than micrometer-scaled emulsified droplets. The emulsification procedure, which

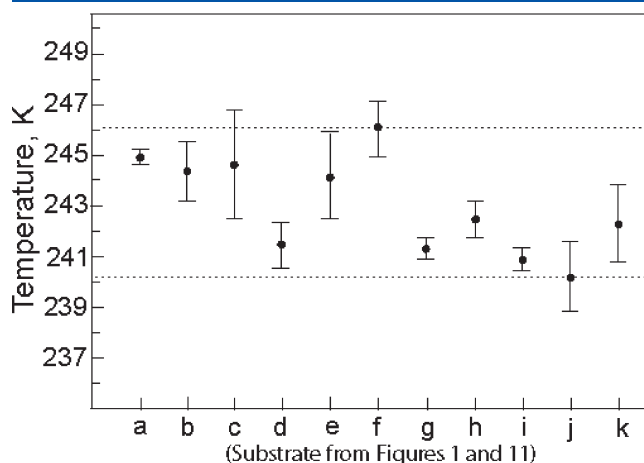


**Figure 3.** Average temperatures of the freezing out of ice,  $T_{\text{ice},n}^{\text{avr}}$ , and standard deviation,  $\sigma_n$ , calculated for each substrate in Figure 1. The letter k denotes the substrate of the semifluorinated block copolymer (see section 3.10).

**Table 1.** Average Temperatures of the Freezing Out of Ice,  $T_{\text{ice},n}^{\text{avr}}$ , Standard Deviation,  $\sigma_n$ , and the Number of Measurements,  $N$ , Performed on Each Substrate<sup>a</sup>

	a	b	c	d	e	f	g	h	i	j	k
$N$	10	22	8	15	6	8	3	4	9	26	6
$T_{\text{ice},n}^{\text{avr}}$	244.8	244.3	244.6	241.5	244.1	246.1	241.3	242.5	240.9	240.2	242.3
$\sigma_n$	$\pm 0.6$	$\pm 2.4$	$\pm 4.5$	$\pm 1.9$	$\pm 3.7$	$\pm 2.2$	$\pm 0.9$	$\pm 1.5$	$\pm 0.9$	$\pm 2.9$	$\pm 3.1$

<sup>a</sup> The letters correspond to the substrates depicted in Figure 1a–j, respectively. The letter k denotes the substrate of the semifluorinated block copolymer (see section 3.10).

produces a huge number of droplets, segregates and isolates immersed foreign ice nuclei within the small fraction of droplets. Because emulsified droplets are isolated from each other by the oil/surfactant matrix, the majority of droplets freeze homogeneously (if there is no interaction between liquid and surfactant). Only those droplets, containing ice nuclei, will freeze heterogeneously at warmer temperature. In our case, below, we will consider two situations of the freezing of droplets. (i) We assume that the heterogeneous freezing of our droplets is initiated solely by substrates because our 25 wt %  $(\text{NH}_4)_2\text{SO}_4$  solution is prepared using ultrapure deionized water and 99.99%  $(\text{NH}_4)_2\text{SO}_4$  crystals. (ii) We also consider a situation when the freezing of droplets is triggered by rare solid dust particles that may exist in droplets despite the considerable purity of the water and ammonium sulfate. It had been reported some time ago that, even if considerable care is taken, such solid nuclei still may exist.<sup>28</sup>

On substrates, the freezing out of pure ice is initiated heterogeneously by ice nucleating sites that can be seen as configurations of surface electrical fields capable of reducing an energy barrier needed for the formation of a critical ice embryo. The ice nucleating sites possess different ice nucleation efficiencies; that is, they can initiate ice nucleation at different temperatures. On solids, in our case of Au and Al ( $\text{Al}_2\text{O}_3$ ) surfaces, the ice-nucleation-favorable electrical fields can be formed around cracks, dislocations, structure irregularities, etc.<sup>4</sup> On the dense films of lanolin wax and halocarbon grease, they can be formed by the complex surface topology and, in the case of mineral and halocarbon oils and the four oil/surfactant mixtures, by a particular arrangement of surface long-chain organic molecules. Usually, substrates of different surface properties possess different densities of ice nucleating sites of different ice nucleating efficiencies.<sup>4</sup> If so, then in Figures 1 and 3, one would expect not only different scattering of individual  $T_{\text{ice}}$ 's but also the different values of  $T_{\text{ice},n}^{\text{avr}}$ . However, as is indicated above, the situation is not as expected: the measured  $T_{\text{ice},n}^{\text{avr}}$ 's are quite similar, and the difference between the warmest and coldest values is only  $\sim 6$  K, as is seen in Figure 3.

To account for the quite similar heterogeneous  $T_{\text{ice},n}^{\text{avr}}$ 's obtained on the substrates of different surface properties, we put forward a hypothesis that  $\text{NH}_4^+$  and  $\text{SO}_4^{2-}$  ions adsorb at the solution/substrate interfaces and modify ice-nucleation-favorable electrical fields. In this case, the interaction of the modified electrical fields with polar  $\text{H}_2\text{O}$  molecules will govern ice nucleation and, consequently,  $T_{\text{ice}}$ . The adsorbed  $\text{NH}_4^+$  and  $\text{SO}_4^{2-}$  may neutralize the "warm" ice nucleation sites that would even out the ice nucleating efficiency of the solution/substrate interface. The evened out ice nucleation efficiencies would produce similar  $T_{\text{ice},n}^{\text{avr}}$ 's and less scattered individual  $T_{\text{ice}}$ 's, which are seen in the majority of panels in Figure 1. The neutralization of warm ice nucleation sites may result in the colder average  $T_{\text{ice},n}^{\text{avr}}$  in comparison with the average freezing temperatures of pure water droplets,  $T_{\text{ice},w}^{\text{avr}}$ , as is seen from the comparison of Figures 1 and 4. In Figure 4, the thermograms of pure water droplets placed on Al ( $\text{Al}_2\text{O}_3$ ) and halocarbon grease are shown. It is seen that both substrates produce almost the same heterogeneous freezing temperature of  $T_{\text{ice},w}^{\text{avr}} \approx 251$  K. Of course, the colder  $T_{\text{ice},n}^{\text{avr}}$  in comparison with the  $T_{\text{ice},w}^{\text{avr}}$  can be partly accounted for by the presence of  $(\text{NH}_4)_2\text{SO}_4$ , which increases the supersaturation required for ice nucleation to occur when compared to pure water. An aspect to note is that the scattering of the individual  $T_{\text{ice},w}$ 's around the  $T_{\text{ice},w}^{\text{avr}}$  is similar to the scattering of  $T_{\text{ice}}$ 's presented in Figure 1b,e. These results

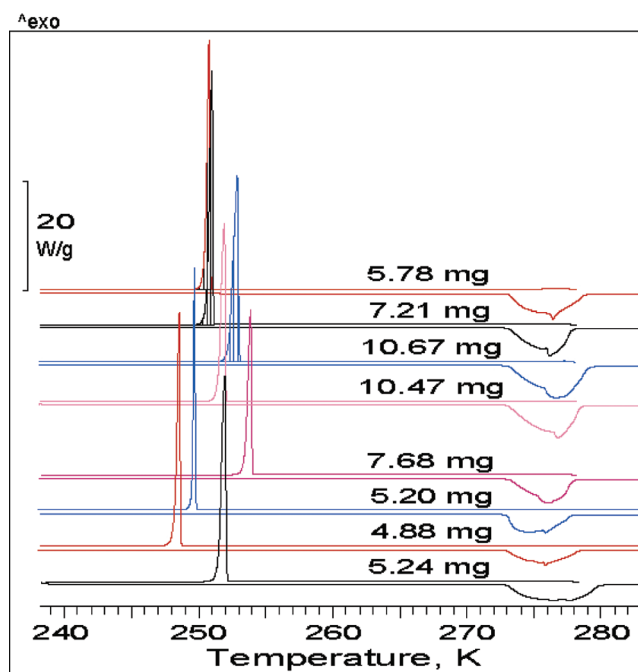


**Figure 4.** DSC thermograms obtained from eight ultrapure water droplets placed on the substrates of Al ( $\text{Al}_2\text{O}_3$ ) (upper four thermograms) and halocarbon grease (lower four thermograms). Numbers denote the mass of droplets. Cooling and warming scanning rates are 3 K/min. The scale bar indicates the heat flow through droplets.

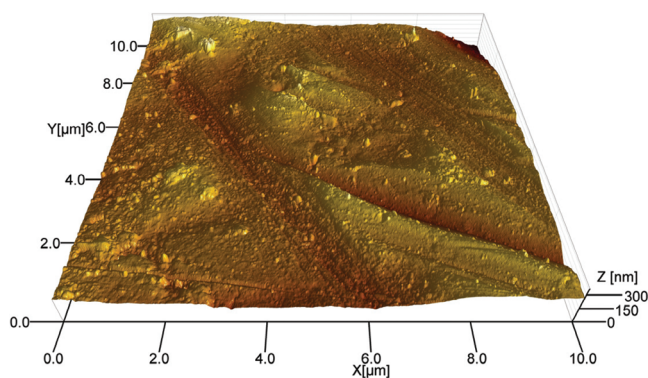


**Figure 5.** Atomic force microscopy (AFM) image of the surface of the Al ( $\text{Al}_2\text{O}_3$ ) DSC crucible.

seem to contradict the above-proposed hypothesis. However, one may assume that the roughness over a  $1 \mu\text{m}^2$  of solid Al ( $\text{Al}_2\text{O}_3$ ) and dense grease is large and the adsorbed  $\text{NH}_4^+$  and  $\text{SO}_4^{2-}$  may not sufficiently even out their ice nucleating efficiency, which may result in the similar scattering of the  $T_{\text{ice},w}$ 's and  $T_{\text{ice}}$ 's. Indeed, an atomic force microscopy (AFM) image of the surface of the Al crucible shown in Figure 5 demonstrates that the surface topology of the Al ( $\text{Al}_2\text{O}_3$ ) surface is complex and the roughness over a  $1 \mu\text{m}^2$  is quite large.

An alternative explanation of the quite similar heterogeneous  $T_{\text{ice},n}^{\text{avr}}$  is based on the presence of nanometer-sized dust ice nuclei immersed into 25 wt %  $(\text{NH}_4)_2\text{SO}_4$  droplets. We mentioned above that, even if considerable care is taken, such solid dust ice nuclei still may exist in solution droplets.<sup>28</sup> The most effective immersed dust ice nucleus can trigger the freezing out of

ice in the whole droplet. If so, then the droplets placed on the substrates of a–k (see Figures 1 and 3) should contain at least one such effective nucleus whose ice nucleating efficiency is in the temperature region shown in Figure 3. The ice nucleating efficiency of the nucleus should be “warmer” or at least similar to the ice nucleating efficiency of surface ice nucleating sites of any substrate, including the Al ( $\text{Al}_2\text{O}_3$ ) substrate. However, Figure 5 demonstrates that the very rough surface of the Al ( $\text{Al}_2\text{O}_3$ ) substrate can possess a variety of ice nucleating sites whose ice nucleating efficiency can vary in large limits. It looks unlikely that 25 wt %  $(\text{NH}_4)_2\text{SO}_4$  droplets produced of ultrapure water and 99.99%  $(\text{NH}_4)_2\text{SO}_4$  crystals would uptake dust ice nuclei of “warm” and *uniform-ice-nucleating-efficiency* from laboratory air. The time of solution preparation is about 1–2 min, which includes the weighing of solid  $(\text{NH}_4)_2\text{SO}_4$  and addition of  $\text{H}_2\text{O}$ . The time needed for the loading of droplets into DSC crucibles is  $\sim 15$  s (see the Experimental Section). However, we do not rule out the second explanation which, similar to the first one, is also hypothetical and needs experimental verification. To verify the validity of the discussed above two approaches, further study is needed. For the time being, our aim in this section is to present a new idea that the adsorbed ions of the solute may neutralize and modify surface ice nucleating sites on the solution/substrate interface.

Physically, the neutralization of warm ice nucleation sites and the concomitant evening out of their ice nucleation efficiency can be due to the formation of multimolecular ions/ $\text{H}_2\text{O}$  layers near the substrates.  $\text{H}_2\text{O}$  molecules in the vicinity of the adsorbed  $\text{NH}_4^+$  and  $\text{SO}_4^{2-}$  ions are in a more ordered arrangement than in bulk. The probability of ice nucleation within the ordered  $\text{H}_2\text{O}$  is smaller than that in disordered  $\text{H}_2\text{O}$  because of the additional energy needed for the rearrangement of  $\text{H}_2\text{O}$  molecules into the icelike structure of a critical ice embryo.<sup>4</sup> As a result, the heterogeneous freezing of aqueous solutions occurs at colder temperature than the heterogeneous freezing of pure water. Of course, as we mentioned above, the presence of solute increases ice supersaturation required for ice nucleation to occur when compared to pure water supersaturation.

The small difference between the  $T_{\text{ice},n}^{\text{avr}}$  of the “warm” and “cold” groups of substrates seen in Figure 3 may be accounted for as follows. The OH functional groups of surfactants are directed toward solution and form a uniform surface electrical potential. Therefore, the molecular layers of liquid adjacent to the oil/surfactant mixtures would be in a more ordered arrangement than the molecular layers adjacent to the substrates of the cold group. The more ordered molecular arrangement can be a reason that the average freezing temperatures obtained on the d, g, h, i, j, and k substrates (see Figure 3) are slightly colder than those obtained on the other five substrates of a, b, c, e, and f.

**3.3. Two Stages of the Freezing Out of Pure Ice.** Figure 6 presents the 20-fold magnification of thermograms obtained from 25 wt %  $(\text{NH}_4)_2\text{SO}_4$  droplets placed on hydrophilic halocarbon oil and hydrophobic lanolin substrates. The magnified thermograms obtained from the droplets placed on other substrates are similar. The small exothermic and endothermic peaks at  $\sim 223$  K are due to para-to-ferroelectric ( $\text{P} \rightarrow \text{F}$ ) and ferro-to-paraelectric ( $\text{F} \rightarrow \text{P}$ ) transitions that occur in crystalline  $(\text{NH}_4)_2\text{SO}_4$ .<sup>13</sup> In Figure 6a, the upper two thermograms are obtained from the same droplet with the time interval of 64 days between the two measurements. It is seen that the thermograms are practically identical; that is, the smooth inert substrate of halocarbon oil does not impact on the freezing behavior of the

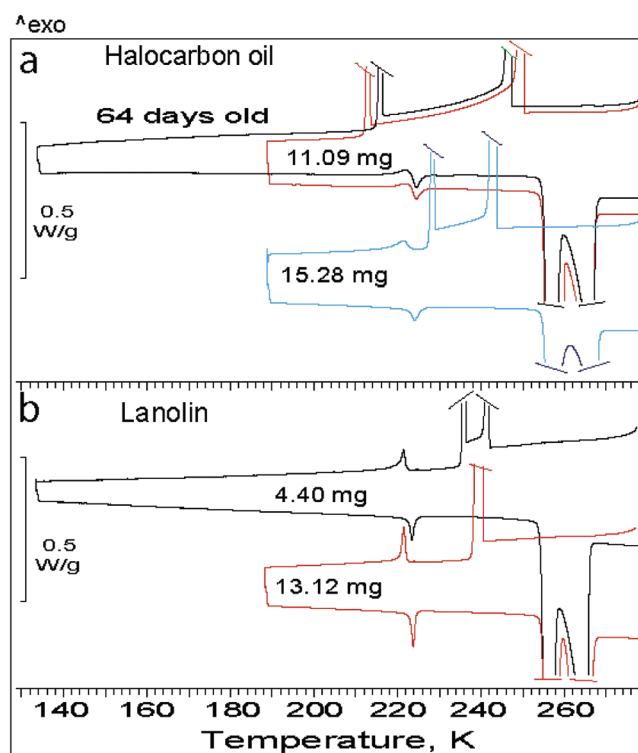


**Figure 6.** Twenty-fold magnification of the thermograms of 25 wt %  $(\text{NH}_4)_2\text{SO}_4$  droplets placed on (a) hydrophilic halocarbon oil and (b) hydrophobic lanolin wax. In panel (a), the two upper thermograms were obtained from the same droplet: the truncated red thermogram from the fresh droplet and the complete black thermogram from the 64 day-old droplet. The para-to-ferroelectric ( $\text{P} \rightarrow \text{F}$ ) and ferro-to-paraelectric ( $\text{F} \rightarrow \text{P}$ ) transitions in crystalline  $(\text{NH}_4)_2\text{SO}_4$  at  $\sim 223$  K are seen in the cooling and warming thermograms, respectively.<sup>13</sup> The numbers denote the mass of droplets. The cooling/warming rate is 3 K/min.

droplet. The effect of the aging of the solution/substrate interface on the appearance of  $T_{\text{ice}}$  and  $T_{\text{res}}$  will be discussed in section 3.6.

Figure 6 shows that the slope and height of the part of thermograms between  $T_{\text{ice}}$  and  $T_{\text{res}}$  differ from those prior to the  $T_{\text{ice}}$  and after the  $T_{\text{res}}$ . The parts of the thermograms prior to the  $T_{\text{ice}}$  and after the  $T_{\text{res}}$  are straight lines (baselines) that do not contain any exothermic transition peak(s) and/or a step of glass transition. The part of the thermogram between the  $T_{\text{ice}}$  and  $T_{\text{res}}$  is higher and inclined from the  $T_{\text{ice}}$  to the  $T_{\text{res}}$ . The presence of the inclined thermogram indicates that the freezing out of pure ice proceeds in two stages. During the first fast stage, which produces the large peak at  $T_{\text{ice}}$ , the majority of ice is rapidly formed. During this stage, the concentration of the rejected  $\text{NH}_4^+$  and  $\text{SO}_4^{2-}$  ions in the residual solution increases rapidly. During the second sluggish stage, which is between the  $T_{\text{ice}}$  and  $T_{\text{res}}$ , the freezing out of ice gradually continues and the concentration of the residual solution slightly increases. Figure 6 also shows that the duration of the sluggish stage can be different. In the case when the two freezing events partly overlap, the sluggish stage is absent, as is seen in the lower red cooling thermogram in Figure 6b. The larger the duration of the sluggish stage is the higher the concentration of a residual solution. More about the concentration of the residual solution will be given in section 3.7.

As is seen in Figure 6, the height of the baseline is different before and after the freezing and melting transitions. The different heights of the baselines are due to the fact that the heat

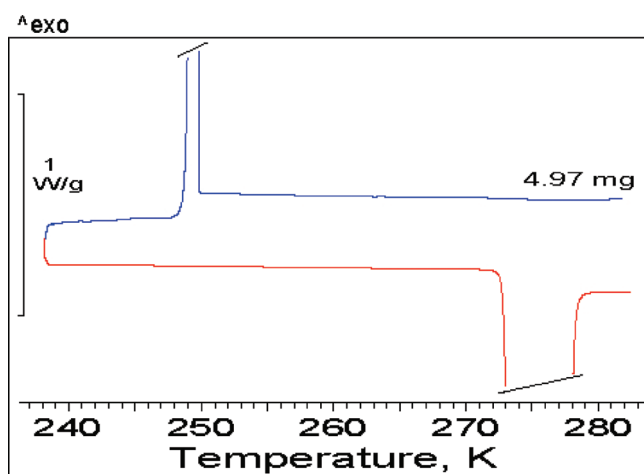


**Figure 7.** Fifty-fold magnification of the cooling (upper blue) and warming (lower red) thermograms of a pure water droplet. The thermograms show the change of the height of the baseline before and after the freezing and melting transitions. The droplet is placed on the Al ( $\text{Al}_2\text{O}_3$ ) substrate. The onset of freezing is at  $\sim 250$  K. The exothermic freezing and endothermic melting peaks are truncated to fit the figure. The mass of droplets is 4.97 mg. The cooling/warming rate is 3 K/min.

capacity,  $C_p$ , of the droplets changes during the first-order phase transitions.<sup>29</sup> In Figure 7, the difference of the height of baselines before/after the freezing/melting transition is shown for a pure water droplet. Because the heat capacity of ice<sup>30</sup> is smaller than that of liquid water,<sup>31</sup> the height of the baseline lowers during freezing and increases during melting. Figure 6 shows that the height of the parts of thermograms corresponding to mixed-phase droplets (between the  $T_{\text{ice}}$  and  $T_{\text{res}}$ ) is higher than that of the unfrozen droplets. This means that latent heat is also produced in the second, sluggish part. The latent heat production ceases slowly (inclined part between the  $T_{\text{ice}}$  and  $T_{\text{res}}$ ), and after some time, it can no longer be detected. In the absence of latent heat production, the baseline reflects the heat capacity of the mixed-phase droplets, which is in between the heat capacity of the unfrozen solution and the heat capacity of the completely frozen droplets. Between  $\sim 240$  and 220 K (Figure 6a), the “apparent” heat capacity (containing the latent heat contribution) is still higher than the heat capacity of the liquid droplet, which indicates that ice slowly precipitates in the whole temperature range. Note that the heat capacity is also slightly changed during the  $\text{P} \rightarrow \text{F}$  and  $\text{F} \rightarrow \text{P}$  transitions in crystalline  $(\text{NH}_4)_2\text{SO}_4$ .

**3.4. Impact of Substrates on  $T_{\text{res}}$ .** The impact of the surface properties of substrates on  $T_{\text{res}}$  has not been studied before because the existence of the two freezing events in millimeter-scaled  $(\text{NH}_4)_2\text{SO}_4/\text{H}_2\text{O}$  droplets has been found only recently.<sup>13</sup> Earlier, even three freezing events were detected during the cooling of small  $(\text{NH}_4)\text{HSO}_4/\text{H}_2\text{O}$  solution samples.<sup>32,33</sup> It was also reported that two or three freezing events appear during the cooling of micrometer-scaled emulsified binary and multicomponent aqueous droplets.<sup>5,25,32</sup> The understanding of the impact of substrates on  $T_{\text{res}}$  of aqueous droplets can be useful, for example, for cloud physics. It is believed that, in the atmosphere, cirrus ice clouds may be formed by both homogeneous and heterogeneous freezing of aqueous droplets, including  $(\text{NH}_4)_2\text{SO}_4/\text{H}_2\text{O}$ .<sup>34–37</sup> The knowledge of whether, at atmospheric temperatures, the atmospheric ice nuclei induce one freezing event, of  $T_{\text{ice}}$ , or two, of  $T_{\text{ice}}$  and  $T_{\text{res}}$ , is

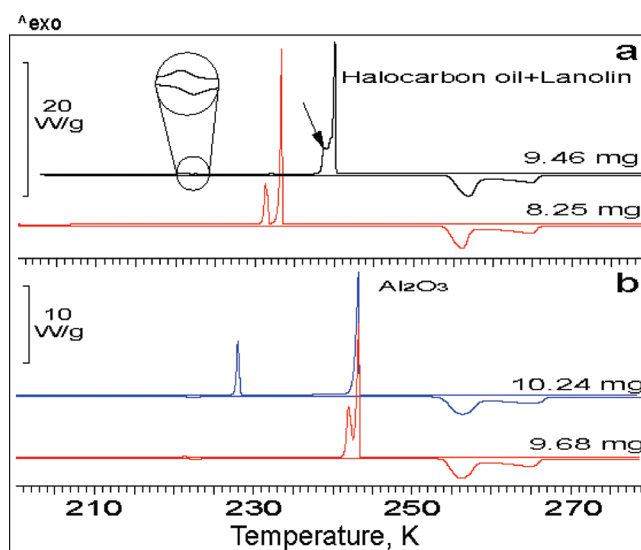


**Figure 8.** Examples of thermograms in which  $T_{\text{res}}$  is outside the region of 210–225 K (see text for details). (a) Thermograms obtained from two droplets placed on a halocarbon oil + lanolin mixture. (b) Thermograms obtained from two droplets placed on Al ( $\text{Al}_2\text{O}_3$ ). The mass of droplets is indicated. The arrow points to the freezing peak of the residual solution. The magnified parts show  $\text{P} \rightarrow \text{F}$  and  $\text{F} \rightarrow \text{P}$  transitions at  $\sim 223$  K in the cooling and warming thermograms, respectively.<sup>13</sup> The cooling/warming rate is 3 K/min.

important because, in the former case, cirrus particles would be mixed-phased and, in the latter case, completely solid. The different phase states of cirrus ice particles can impact differently the atmospheric physical and chemical processes (the rate of heterogeneous reactions destructing the upper tropospheric (UT) ozone, the uptake of moisture by cloud particles in the UT, the radiative properties of cirrus, etc.), which ultimately may impact the climate.<sup>5,24,25</sup>

The scattering of  $T_{\text{res}}$ 's is larger than that of  $T_{\text{ice}}$ 's, as is seen in Figure 1.  $T_{\text{res}}$  is encountered in the immediate vicinity of the corresponding  $T_{\text{ice}}$  (the blue thermogram in Figure 1a and the black one in Figure 1b) and can be more than 30 K colder than  $T_{\text{ice}}$  (the red thermogram in Figure 1b). The large scattering of  $T_{\text{res}}$ 's leads us to an important conclusion, namely, that ice, which is always in contact with the residual solution (see Figure 2), does not trigger heterogeneous freezing of the residual solution. If it were triggering it, then the scattering of  $T_{\text{res}}$ 's would have been much smaller or even absent.

The analysis of numerous thermograms (also those not presented in Figure 1) indicates that, excluding the measurements on lanolin wax (Figure 1d) and the two oil/lanolin mixtures (Figure 1i,j), the majority of  $T_{\text{res}}$ 's falls in a temperature region of  $\sim 210$ –225 K. A small part of all measured  $T_{\text{res}}$ 's (less than  $\sim 20\%$ ) falls in between this region and the corresponding  $T_{\text{ice}}$ 's. The examples of thermograms in which  $T_{\text{res}}$ 's are in between the  $\sim 210$ –225 K region and the corresponding  $T_{\text{ice}}$ 's are shown in Figure 1a,b,d,e,f. In rare cases, the freezing peaks of  $T_{\text{res}}$  and  $T_{\text{ice}}$  can strongly overlap, as is seen in Figure 8. However, for all substrates, we have never obtained thermograms in which the two freezing events overlap completely, that is,  $T_{\text{ice}} - T_{\text{res}} > 0$ . This is understandable because the nucleation and subsequent crystallization of solid require supersaturation. Ammonium sulfate remains unsupersaturated at  $T_{\text{ice}}$ , because the solubility line of  $(\text{NH}_4)_2\text{SO}_4$  is very steep, and therefore, the 25 wt %

$(\text{NH}_4)_2\text{SO}_4$  concentration is far on the left side of the solubility line extrapolated to low temperature (see Figure 10 and section 3.7). The measurements of 25 wt %  $(\text{NH}_4)_2\text{SO}_4$  droplets show that, independent of the surface properties of the studied substrates, the majority of  $T_{\text{res}}$ 's tends to fall into the temperature region of  $\sim 210\text{--}225$  K. This result is similar to that found for 5–38 wt %  $(\text{NH}_4)_2\text{SO}_4$  droplets placed on Al ( $\text{Al}_2\text{O}_3$ ).<sup>14</sup> The fact that the residual  $(\text{NH}_4)_2\text{SO}_4/\text{H}_2\text{O}$  solution tends to freeze in a narrow temperature region is not unique. A residual solution formed after the freezing out of pure ice in micrometer-scaled emulsified  $\text{H}_2\text{SO}_4/\text{H}_2\text{O}$  droplets also freezes in a narrow temperature region (see Figure 1 in ref 38).

The tendency of  $T_{\text{res}}$  to occupy a relatively narrow temperature region may be accounted for by the fact that the concentration of the residual  $(\text{NH}_4)_2\text{SO}_4/\text{H}_2\text{O}$  solution varies in relatively small limits. The scattering of  $T_{\text{res}}$ 's within the  $\sim 210\text{--}225$  K region may be due to different active sites (different local surface electrical fields) capable of triggering the freezing of the residual solution at different  $T_{\text{res}}$ 's. The rare freezing events, when  $T_{\text{res}}$  and  $T_{\text{ice}}$  partly overlap or  $T_{\text{res}}$  is in close vicinity to the corresponding  $T_{\text{ice}}$ , may be brought about by some specific nuclei (for example, contaminations) capable of inducing the heterogeneous freezing of the residual solution at warmer temperature. The mechanism of the freezing of the residual solution will be discussed in section 3.7.

**3.5. Impact of Lanolin on  $T_{\text{res}}$ .** Figure 1d,i,j demonstrates that the 25 wt %  $(\text{NH}_4)_2\text{SO}_4$  droplets placed on pure lanolin wax and two oil/lanolin mixtures systematically produce  $T_{\text{res}}^{\text{lanolin}}$  warmer than  $T_{\text{res}}$ 's produced by the droplets placed on other substrates. (To distinguish between  $T_{\text{res}}$  obtained on lanolin-containing substrates and that obtained on other substrates, we name the former as  $T_{\text{res}}^{\text{lanolin}}$ ). In a series of 15 measurements performed on lanolin wax (see Table 1), only one measurement gives  $T_{\text{res}}^{\text{lanolin}}$  in the region of  $\sim 210\text{--}225$  K (blue cooling thermogram in Figure 1d). In a series of 35 measurements performed on the two oil/lanolin mixtures, all  $T_{\text{res}}^{\text{lanolin}}$  are warmer than the region of  $\sim 210\text{--}225$  K (Figure 1i,j). For example, the  $T_{\text{res}}^{\text{lanolin}}$ 's obtained on the mineral oil/lanolin mixture are between 228 and 233 K and, on halocarbon-oil/lanolin mixture, between 230 and 235 K. Although the difference is small, it nevertheless is clearly detectable and suggests that the type of oil may also impact the  $T_{\text{res}}$ 's. However, in contrast to the lanolin-containing mixtures, the measurements of the droplets placed on the two Span65-containing mixtures produce  $T_{\text{res}}$ 's that are well within the region of  $\sim 210\text{--}225$  K (Figure 1g,h). Thus, the analysis of panels d and g–i in Figure 1 (and also thermograms not shown in Figure 1) indicates that the surfactant and, to a lesser degree, the oil can change the  $T_{\text{res}}$ 's of the residual solution.

The warmer  $T_{\text{res}}^{\text{lanolin}}$ 's obtained on the lanolin-containing substrates suggest that the interaction between  $\text{NH}_4^+$ ,  $\text{SO}_4^{2-}$ , and lanolin may be stronger than the interaction between  $\text{NH}_4^+$ ,  $\text{SO}_4^{2-}$ , and other substrates. As reported in the Experimental Section, lanolin consists of cholesterol, wool alcohols, and the esters derived from several fatty acids. The ions of  $\text{NH}_4^+$  and  $\text{SO}_4^{2-}$  may interact more strongly with the functional groups of these organic substances than with other substrates. However, the strong interaction does not involve a chemical reaction, which would produce a new substance (product). The magnification of low-temperature thermograms down to 133 K does not reveal any new transition peak(s) that would characterize the phase transitions associated with the newly formed substance. Also, as indicated in section 3.1, the overall concentration of

droplets of 25 wt %  $(\text{NH}_4)_2\text{SO}_4$  is not changed on the time-scale of measurements of less than 2 h. This is inferred from the fact that the melting point of ice of  $T_{\text{ice,m}} \approx 265$  K is constant. Whether there is a slow reaction, which could manifest itself on the large time-scales, is discussed in the next subsection.

**3.6. Impact of Aged Solution/Lanolin Interface on  $T_{\text{res}}^{\text{lanolin}}$ .** One may assume that a possible slow reaction of  $\text{NH}_4^+$  and  $\text{SO}_4^{2-}$  with lanolin could be detected on the time-scale much larger than 2 h. In this case, the reaction could manifest itself by the change of the overall concentration of droplets and/or by the appearance of new transition event(s) in the corresponding thermograms. The change of the overall concentration of “aged” droplets would necessarily change the melting temperature of ice,  $T_{\text{ice,m}}$ , in the “aged” thermograms in comparison with the  $T_{\text{ice,m}}$  in the “fresh” thermograms. In Figure 6a, the fresh and aged, 64 day-old thermograms obtained from the same droplet placed on halocarbon oil are shown. Because halocarbon oil is chemically inert to practically all acids, alkalis, and oxidizing agents (see Experimental part), the aged thermograms contain no evidence of any new transition events or the change of the overall concentration.

To verify whether a slow reaction of  $\text{NH}_4^+$  and  $\text{SO}_4^{2-}$  with lanolin exists or not, we performed a series of double measurements of the same 25 wt %  $(\text{NH}_4)_2\text{SO}_4$  droplets placed on lanolin wax and halocarbon oil/lanolin mixtures. The first measurements were performed on “fresh” droplets and the second ones on “aged”, more than 2.5 months old, droplets. Figure 9 is presented to demonstrate the comparison of fresh and aged thermograms. It is seen that, in the aged thermograms, (i) there is no additional freezing/melting event and (ii) the peak melting temperature of ice,  $T_{\text{ice,m}} \approx 265$  K, is the same as in the fresh thermograms. The latter means that the overall concentration of droplets is not changed during the aging period of more than 2.5 months. Figure 9 also shows that the position of  $T_{\text{res}}^{\text{lanolin}}$  in the aged thermograms can be changed (Figure 9a, b) and unchanged (Figure 9c) relative to the position of  $T_{\text{res}}^{\text{lanolin}}$  in fresh thermograms. The analysis of the aged thermograms also shows that  $T_{\text{res}}^{\text{lanolin}}$ 's do not jump below 210 K (i.e., in the  $\sim 210\text{--}225$  K region). The similarity of the scattering of aged and fresh  $T_{\text{res}}^{\text{lanolin}}$ 's suggests that the aging of 25 wt %  $(\text{NH}_4)_2\text{SO}_4$  droplets does not change the concentration of the residual solution too; that is, the shift of  $T_{\text{res}}^{\text{lanolin}}$  to warmer temperatures is independent of the aging of the solution/lanolin interface. The above discussion indicates that there is no slow reaction of  $\text{NH}_4^+$  and  $\text{SO}_4^{2-}$  ions with lanolin. Therefore, most probably, the interaction between  $\text{NH}_4^+$  and  $\text{SO}_4^{2-}$  ions and lanolin is simply physical adsorption, not a chemical reaction.

**3.7. What Drives  $T_{\text{res}}^{\text{lanolin}}$  to Warmer Temperature?** The nature of the mechanism that drives  $T_{\text{res}}^{\text{lanolin}}$  to warmer temperatures is not completely clear. We propose the following explanation. Our previous measurements<sup>14</sup> show that  $T_{\text{ice,S-38 wt \%}}$  of millimeter-scaled droplets placed on the Al ( $\text{Al}_2\text{O}_3$ ) substrate decreases with increasing concentration from 5 to 38 wt %  $(\text{NH}_4)_2\text{SO}_4$ . In Figure 10, the transition temperatures of  $T_{\text{ice,m,5-38 wt \%}}$ ,  $T_{\text{ice,S-38 wt \%}}$ , and  $T_e$  taken from ref 14 and the freezing temperatures of emulsified  $(\text{NH}_4)_2\text{SO}_4/\text{H}_2\text{O}$  droplets,  $T_{\text{f,emul}}$ , taken from ref 12 are superimposed on the phase diagram of  $(\text{NH}_4)_2\text{SO}_4/\text{H}_2\text{O}$ .<sup>27</sup> The  $T_{\text{f,emul}}$ 's are supposed to be homogeneous freezing temperatures of micrometer-scaled droplets and presented for comparison. Also shown by the filled dots are  $T_{\text{res}}^{\text{lanolin}}$ 's taken from Figure 1i,j (see section 3.5). The volume of 25 wt %  $(\text{NH}_4)_2\text{SO}_4$  droplets and the volume of the residual



According to this approach, the intersection points of the purple region with the EC line would give the concentration region of the residual solution between  $\sim 55$  and  $59$  wt %  $(\text{NH}_4)_2\text{SO}_4$ , as is shown by the dotted lines. Similarly, the concentration region of the residual solution that freezes in the  $\sim 210$ – $225$  K region would be between  $\sim 61$  and  $66$  wt %  $(\text{NH}_4)_2\text{SO}_4$ . Thus, the latter approach gives higher concentrations than our approach.

The latter approach seems preferable because our approach suffers from one drawback: the two freezing events, namely,  $T_{\text{ice}}$  and  $T_{\text{res}}^{\text{lanolin}}$ , are assumed to be on the  $T_{\text{ice},5-38}$  wt % curve. However, these freezing events are different. The first freezing event produces a phase separation into pure ice and the residual solution, that is, the separation into solid and liquid phases, whereas during the second freezing event,  $T_{\text{res}}^{\text{lanolin}}$ , there is no phase separation because the residual solution completely freezes to the solid phase. If, according to our approach, the concentration of the residual solution is indeed between  $\sim 35$  and  $40$  wt %  $(\text{NH}_4)_2\text{SO}_4$  (or between  $\sim 33$  and  $38$  wt %  $(\text{NH}_4)_2\text{SO}_4$ ; see above), then, according to Figure 10 (or ref 14), the residual solution with a concentration less than  $38$  wt %  $(\text{NH}_4)_2\text{SO}_4$  should produce two freezing events. However, it does not. This fact may be considered in favor of the second approach; that is, the concentration of the residual solution of  $25$  wt %  $(\text{NH}_4)_2\text{SO}_4$  droplets might be much higher than  $40$  wt %  $(\text{NH}_4)_2\text{SO}_4$ . Here, it should be recalled that the concentration of the residual solution was assumed to be  $\sim 40$  wt %  $(\text{NH}_4)_2\text{SO}_4$ , independent of the overall concentration of the droplets. This was inferred from the onset of the eutectic melting.<sup>13</sup> The above discussion suggests that the concentration of the residual solution cannot be determined solely from the eutectic melting point. Further measurements and calculations are needed in order to get insight into the concentration of the residual solution formed after the freezing out of pure ice.

**3.8. How Does the Residual Solution Freeze?** Figure 10 shows that the second approach prescribes for the above-discussed two residual solutions the concentrations as high as  $\sim 55$ – $59$  and  $\sim 61$ – $66$  wt %  $(\text{NH}_4)_2\text{SO}_4$ . These concentrations are much higher than the concentration corresponding to the  $(\text{NH}_4)_2\text{SO}_4$  solubility line extrapolated to low temperature (the line EB in Figure 10). It looks unlikely that such high concentrations can be reached at low temperature. One would expect the crystallization (precipitation) of pure  $(\text{NH}_4)_2\text{SO}_4$  crystals from the highly supersaturated residual solution. It has been reported that the crystallization of solely solute from the freeze-concentrated residual solution may occur instead of the freezing of the whole residual solution.<sup>22</sup> The precipitation of  $(\text{NH}_4)_2\text{SO}_4$  crystals could have resulted in the appearance of a third exothermic event in between  $T_{\text{ice}}$  and  $T_{\text{res}}$ . However, the magnification of numerous cooling thermograms does not reveal any transition peaks in between  $T_{\text{ice}}$  and  $T_{\text{res}}$ ; see, for example, Figures 6a and 9a,b.

After the precipitation of  $(\text{NH}_4)_2\text{SO}_4$  crystals, one may assume two routes of the freezing of the residual solution. (i) The precipitation of  $(\text{NH}_4)_2\text{SO}_4$  crystals will lead to the reduction of the concentration or, with the analogy of the freezing out of pure ice, to the formation of a new “freeze-reduced-concentrated” residual solution, which would immediately freeze, to form again a freeze-concentrated residual solution! The succession of such freezing events would have resulted in a broad, uneven second freezing peak in cooling thermograms. However, we never observed such uneven second freezing peaks. Instead, they have a smooth, usually bell-shaped form, that indicates a single freezing process. (ii) The precipitated (nucleated)

$(\text{NH}_4)_2\text{SO}_4$  crystal may immediately trigger the nucleation of adjacent pure ice crystal(s). It has been reported that  $(\text{NH}_4)_2\text{SO}_4$  microcrystals are good ice nucleating agents.<sup>34</sup> The growth of  $(\text{NH}_4)_2\text{SO}_4$  and ice would proceed simultaneously until all residual solution freezes. However, this mechanism cannot account for those rare situations in which the residual solution starts to freeze despite that the freezing out of ice is not finished yet (see Figure 8.) In this case, the formation of the residual solution is not finished and it is not supersaturated yet. In section 3.4, we suggested that such freezing events could be caused by some specific nuclei (contaminations) capable of inducing the heterogeneous freezing of the residual solution at warmer temperature. In accordance with the above-discussed second route of the freezing of the residual solution, the specific nuclei should trigger the nucleation of  $(\text{NH}_4)_2\text{SO}_4$ . Such nuclei or nucleating sites may exist on a substrate with which the residual solution is in contact, as is schematically shown in Figure 2.

**3.9. Implication for Freezing Emulsions.** The findings that the lanolin-containing substrates slightly reduce  $T_{\text{ice}}$  (see Figure 3) and enhance the corresponding  $T_{\text{res}}^{\text{lanolin}}$  (Figure 1i,j) may have implication for the study of the freezing behavior of micrometer-scaled emulsified aqueous droplets. The oil/surfactant matrix is thought not to impact the freezing behavior of emulsified pure water droplets; that is, it is believed that emulsified water droplets freeze homogeneously. This belief was transferred on the freezing of emulsified solution droplets.<sup>22</sup> However, to the best of our knowledge, to support the transfer, no investigation of the impact of the oil/surfactant matrix on the freezing behavior of aqueous droplets was performed.

Although the exact mechanisms of the approaching of  $T_{\text{ice}}$  and  $T_{\text{res}}^{\text{lanolin}}$  to each other in cooled  $25$  wt %  $(\text{NH}_4)_2\text{SO}_4$  droplets placed on the lanolin-containing substrates are not known with certainty, it is clear that they are happening at the solution/lanolin interface. Therefore, one may assume that, if the area of the interface increases, then the impact on the  $T_{\text{ice}}$  and  $T_{\text{res}}^{\text{lanolin}}$  would be larger. The area of the interface would be largest if droplets are immersed into an oil/lanolin mixture, that is, in an emulsion. As the size of emulsion droplets decreases, the surface-to-volume ratio increases. As a result, the area of the solution/lanolin interface increases and, consequently, its impact on the approaching of  $T_{\text{ice}}$  and  $T_{\text{res}}^{\text{lanolin}}$  to each other would also increase. Earlier, it has been reported that the cooling of micrometer-scaled emulsified  $(\text{NH}_4)_2\text{SO}_4/\text{H}_2\text{O}$  droplets always produces only one freezing event,  $T_{\text{f,emul}}$ .<sup>12,14</sup> In ref 14, the single freezing event has been accounted for by the fact that the  $T_{\text{f,emul}}$  is mainly within the  $\sim 210$ – $225$  K region, as is seen in Figure 10. The approaching of  $T_{\text{ice}}^{\text{lanolin}}$  and  $T_{\text{res}}$  to each other observed in the droplets placed on the lanolin-containing substrates can serve as an additional factor accounting for the single freezing event of emulsified subeutectic  $(\text{NH}_4)_2\text{SO}_4/\text{H}_2\text{O}$  droplets embedded into the halocarbon oil/lanolin matrix. Thus, the above discussion suggests that the lanolin surfactant can impact the freezing behavior of  $(\text{NH}_4)_2\text{SO}_4/\text{H}_2\text{O}$  droplets.

**3.10. Effect of Size on  $T_{\text{res}}$ .** We also investigated the impact of the size (mass) of  $25$  wt %  $(\text{NH}_4)_2\text{SO}_4$  droplets on the distribution of  $T_{\text{ice}}$  and  $T_{\text{res}}$ . It is known that the homogeneous freezing temperature decreases with decreasing size of the solution sample. However, whether heterogeneous  $T_{\text{res}}$  is size-dependent has not been investigated before. The rate of the expulsion of foreign particles (ions) from the ice lattice during the freezing out of pure ice may depend on the size of droplets and, consequently, may impact the formation of the residual solution and,

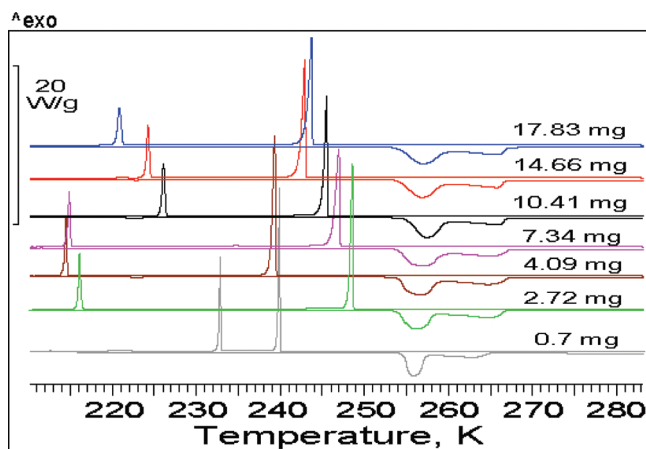


**Figure 11.** Thermograms obtained from 25 wt %  $(\text{NH}_4)_2\text{SO}_4$  droplets of different masses (sizes) placed on a highly hydrophobic film of semifluorinated block copolymer. The numbers denote the mass of droplets. The colder melting temperature of ice in the lowest thermogram of the 0.7 mg droplet is due to the increase of concentration brought about by the evaporation of water during the loading of the droplet into the Al crucible (see text for details). The cooling/warming rate is 3 K/min.

consequently, the appearance of the second freezing event  $T_{\text{res}}$ . To minimize the interaction between the 25 wt %  $(\text{NH}_4)_2\text{SO}_4$  solution and a substrate, we prepared a highly hydrophobic film of semifluorinated block copolymer on the surface of the Al crucible. According to ref 26, the semifluorinated block copolymer has a contact angle for water larger than  $150^\circ$ . In Figure 11, the thermograms obtained from the droplets with a mass between  $\sim 0.7$  and  $\sim 17.83$  mg are presented. It is seen that, despite the 20-fold reduction of mass, there is no pronounced correlation between the appearance of  $T_{\text{ice}}$  and  $T_{\text{res}}$  and the size of droplets. The distribution of  $T_{\text{ice}}$  and  $T_{\text{res}}$  is similar to that presented in Figure 1, excluding panels d, i, and j, in which the shift of  $T_{\text{res}}$  to warmer temperature is due to the interaction of  $\text{NH}_4^+$  and  $\text{SO}_4^{2-}$  ions with lanolin (see above discussion). In the lowest thermogram obtained from the smallest droplet of  $\sim 0.7$  mg,  $T_{\text{ice,mv}}$  is noticeably colder than those in the other thermograms. The colder  $T_{\text{ice,m}}$  means that the concentration of the droplet is higher than 25 wt %  $(\text{NH}_4)_2\text{SO}_4$ . The increase in concentration is due to the evaporation of water during the loading of the small droplet into the DSC crucible (see the Experimental Section). The evaporation is due to the fact that the partial water vapor pressure of the 25 wt %  $(\text{NH}_4)_2\text{SO}_4$  solution is higher than the environmental water pressure. Thus, the 20-fold reduction of the mass of 25 wt %  $(\text{NH}_4)_2\text{SO}_4$  droplets does not impact the appearance of the two freezing events.

#### 4. CONCLUSIONS

This paper presents differential scanning calorimetry (DSC) results of the study of the impact of different substrates on the appearance of two heterogeneous freezing events of millimeter-scaled 25 wt %  $(\text{NH}_4)_2\text{SO}_4$  droplets cooled below the eutectic temperature of  $T_e \approx 254.5$  K. The two freezing events are the heterogeneous freezing out of pure ice,  $T_{\text{ice}}$ , and the subsequent heterogeneous freezing of a residual freeze-concentrated  $(\text{NH}_4)_2\text{SO}_4/\text{H}_2\text{O}$  solution,  $T_{\text{res}}$ . The effect of size and aging of droplets on the appearance of the  $T_{\text{ice}}$  and  $T_{\text{res}}$  has also been

investigated. To this end, we performed numerous DSC measurements of millimeter-scaled 25 wt %  $(\text{NH}_4)_2\text{SO}_4$  droplets placed on 11 substrates with different surface properties. The choice of the droplets of constant concentration was motivated by a desire to investigate a pure effect of substrates, aging, and size on the heterogeneous freezing behavior of  $(\text{NH}_4)_2\text{SO}_4/\text{H}_2\text{O}$  droplets, which otherwise would have been affected by varying concentrations.

The analysis of the obtained DSC thermograms indicates the following: (i) Independent of the surface properties of the substrates, the phase separation into pure ice and a residual freeze-concentrated  $(\text{NH}_4)_2\text{SO}_4/\text{H}_2\text{O}$  solution always occurs during the cooling of 25 wt %  $(\text{NH}_4)_2\text{SO}_4$  droplets below  $T_e$ . In all thermograms,  $T_{\text{ice}}$  always precedes  $T_{\text{res}}$ ; that is, there is always  $T_{\text{ice}} > T_{\text{res}}$ . Our measurements indicate that the appearance of the two freezing events is not due to a specific interaction of  $(\text{NH}_4)_2\text{SO}_4/\text{H}_2\text{O}$  with a particular substrate but due to the intrinsic property of  $(\text{NH}_4)_2\text{SO}_4/\text{H}_2\text{O}$ , which manifests itself as the rejection of  $\text{NH}_4^+$  and  $\text{SO}_4^{2-}$  from the ice lattice during the freezing out of pure ice. (ii) The freezing out of pure ice proceeds in two stages: the fast stage, during which the majority of ice is formed, and the sluggish one, during which the additional amount of ice crystallizes until the residual solution starts freezing. The duration of the sluggish process can impact the concentration of the residual solution. (iii) The average values of  $T_{\text{ice}}$  calculated for more than 10 measurements on each substrate seem not to be strongly governed by the surface properties of the substrates. In addition,  $T_{\text{ice}}$ 's are less sensitive to the surface properties of substrates than the corresponding  $T_{\text{res}}$ . This can be interpreted in the sense that the residual solution also freezes heterogeneously. (iv) The heterogeneous freezing of the residual solution most likely starts from the nucleation of  $(\text{NH}_4)_2\text{SO}_4$  crystals. (v) The interaction of  $\text{NH}_4^+$  and  $\text{SO}_4^{2-}$  with the lanolin surfactant is responsible for the approaching of the transition temperatures of  $T_{\text{ice}}$  and  $T_{\text{res}}$  to each other in comparison with the transition temperatures of the droplets placed on the substrates not containing lanolin. This result serves as evidence that the lanolin surfactant can impact the freezing behavior of emulsified aqueous droplets, at least, emulsified  $(\text{NH}_4)_2\text{SO}_4/\text{H}_2\text{O}$  droplets. It can also serve as an additional factor accounting for the single freezing event that is always observed during the cooling of emulsified  $(\text{NH}_4)_2\text{SO}_4/\text{H}_2\text{O}$  droplets. (vi) The warming thermograms of fresh and aged, more than 2 months, droplets are identical. This indicates that there is no chemical reaction of lanolin with  $\text{NH}_4^+$  and  $\text{SO}_4^{2-}$  ions; that is, the interaction between the ions and lanolin is physical adsorption. (vii) The 20-fold change of the mass of droplets does not impact the appearance of the two freezing events of  $T_{\text{ice}}$  and  $T_{\text{res}}$ .

The DSC results presented in the paper are the first of their kind and can be useful in the different fields of science and experimental situations that deal with the freezing of aqueous systems confined to small dimensions and connected to different surfaces. The presented results can also be useful for the environmental implications, for example, for the atmospheric sciences. Whether the mixed-phased cloud particles (an ice core + a residual solution coating) are formed after the freezing of atmospheric aerosol droplets can have important consequences for the development of high-altitude ice cirrus clouds<sup>5</sup> and PSCs, atmospheric chemistry,<sup>10</sup> and the radiative properties of cirrus.<sup>24</sup> Because cirrus ice clouds are globally widespread and PSCs are believed to be the culprits of the formation of polar stratospheric ozone holes, the microphysics of cirrus and PSCs may be an

important factor impacting the climate and, therefore, should be taken into account in climate models.

## AUTHOR INFORMATION

### Corresponding Author

\*E-mail: anatoli.bogdan@uibk.ac.at.

## ACKNOWLEDGMENT

The authors are thankful for the financial support by the Austrian Science Fund (project P23027) and by the ERC (Starting Grant SULIWA). A.B. thanks F. Klauser for the preparation of the AFM image of the Al surface, S. Lemettinen and E. Kaija for assistance during the performance of DSC measurements, and the Physical and Chemical departments of the University of Helsinki for providing facilities for the performance of DSC measurements.

## REFERENCES

- (1) Baicu, S. C.; Taylor, M. J. *Cryobiology* **2002**, *45*, 33.
- (2) Svishchev, I. M.; Kusalik, P. G. *J. Am. Chem. Soc.* **1996**, *118*, 649.
- (3) Franks, F., Ed. *Water—A Comprehensive Treatise*; Plenum Press: New York, 1982; Vol. 7.
- (4) Pruppacher, H. R.; Klett, J. D. *Microphysics of Clouds and Precipitation*, 2nd ed.; Kluwer: Dordrecht, 1997.
- (5) Bogdan, A.; Molina, M. J. *J. Phys. Chem. A* **2009**, *113*, 14123–14130.
- (6) Takenaka, N.; Ueda, A.; Maeda, Y. *Nature* **1992**, *358*, 736.
- (7) Vaessen, R.; Seckler, M.; Witkamp, G. J. *Ind. Eng. Chem. Res.* **2003**, *42*, 4874.
- (8) Levine, H., Ed. *Amorphous Food and Pharmaceutical Systems*; RSC Publishing: Cambridge, U.K., 2002.
- (9) Bogdan, A. *J. Phys. Chem. B* **2006**, *110*, 12205–12206.
- (10) Bogdan, A.; Molina, M. J.; Tenhu, H.; Mayer, E.; Loerting, T. *Nat. Chem.* **2010**, *2*, 197–201.
- (11) Chang, H.-Y. A.; Koop, T.; Molina, L. T.; Molina, M. J. *J. Phys. Chem.* **1999**, *103*, 2673–2679.
- (12) Bertram, A. K.; Koop, T.; Molina, L. T.; Molina, M. J. *J. Phys. Chem. A* **2000**, *104*, 584–588.
- (13) Bogdan, A. *J. Phys. Chem. A* **2010**, *114*, 10135–10139.
- (14) Bogdan, A.; Molina, M. J.; Tenhu, H.; Mayer, E.; Bertel, E.; Loerting, T. *J. Phys. Condens. Matter* **2011**, *23*, 035103.
- (15) Čolić, M.; Miler, J. D. In *Interfacial Dynamics*; Kallay, N., Ed.; Marcel Dekker Inc.: New York, 2000; p 35.
- (16) Robinson, C.; Boxe, C. S.; Guzman, M. I.; Colussi, A. J.; Hoffmann, M. R. *J. Phys. Chem. B* **2006**, *110*, 7613.
- (17) Schwander, J.; Neftel, A.; Oeschger, H.; Stauffer, B. *J. Phys. Chem.* **1983**, *87*, 4157.
- (18) Takenaka, N.; Ueda, A.; Daimon, T.; Bandow, H.; Dohmaru, T.; Maeda, Y. *J. Phys. Chem.* **1996**, *100*, 13874.
- (19) O'Driscoll, P.; Minogue, N.; Takenaka, N.; Sodeau, J. *J. Phys. Chem. A* **2008**, *112*, 1677.
- (20) Takenaka, N.; Bandow, H. *J. Phys. Chem. A* **2007**, *111*, 8780.
- (21) Killawee, J. A.; Fairchild, I. J.; Tison, J. -L.; Janssens, L.; Lorrain, R. *Geochim. Cosmochim. Acta* **1998**, *62*, 3637.
- (22) Murray, B. J.; Bertram, A. K. *Phys. Chem. Chem. Phys.* **2008**, *10*, 3287–3301.
- (23) Zobrist, B.; Marcolli, C.; Pedernera, D. A.; Koop, T. *Atmos. Chem. Phys.* **2008**, *8*, 5221–5244.
- (24) Räisänen, P.; Bogdan, A.; Sassen, K.; Kulmala, M.; Molina, M. J. *Atmos. Chem. Phys.* **2006**, *6*, 4659–4667.
- (25) Bogdan, A.; Molina, M. J. *J. Phys. Chem. A* **2010**, *114*, 2821–2829.
- (26) Valtola, L.; Koponen, A.; Karesoja, M.; Hietala, S.; Laukkainen, A.; Tenhu, H.; Denifl, P. *Polymer* **2009**, *50*, 3103–3110.
- (27) Beyer, K. D.; Bothe, J. R.; Burrmann, N. *J. Phys. Chem. A* **2007**, *111*, 479–494.
- (28) Pruppacher, H. R.; Neiburger, M. *J. Atmos. Sci.* **1963**, *20*, 376–385.
- (29) Höhne, G.; Hemminger, W.; Flammershain, H.-J. *Differential Scanning Calorimetry*; Springer: Berlin, 1995.
- (30) Angell, C.; Sichina, W.; Oguni, M. *J. Phys. Chem.* **1982**, *86*, 998–1002.
- (31) Haida, O.; Matsuo, T.; Suga, H.; Seki, S. *J. Chem. Thermodyn.* **1974**, *6*, 815–825.
- (32) Koop, T.; Bertram, A. K.; Molina, L. T.; Molina, M. J. *J. Phys. Chem. A* **1999**, *103*, 9042–9048.
- (33) Beyer, K. D.; Bothe, J. *J. Phys. Chem. A* **2006**, *110*, 7105–7112.
- (34) Zuberi, B.; Bertram, A. K.; Koop, T.; Molina, L. T.; Molina, M. J. *J. Phys. Chem. A* **2001**, *105*, 6458–6464.
- (35) Zobrists, B.; Marcolli, C.; Peter, T.; Koop, T. *J. Phys. Chem. A* **2008**, *112*, 3965–3975.
- (36) Oatis, S.; Imre, D.; McGraw, R.; Xu, J. *Geophys. Res. Lett.* **1998**, *25*, 4469–4472.
- (37) Ciobanu, V. G.; Marcolli, C.; Krieger, U. K.; Zuend, A.; Peter, T. *J. Phys. Chem. A* **2010**, *114*, 9486–9495.
- (38) Bogdan, A.; Molina, M. J.; Sassen, K.; Kulmala, M. *J. Phys. Chem. A* **2006**, *110*, 12541–12542.